

Spinodal Decomposition in Binary Gases

S. Bastea and J.L. Lebowitz

Department of Physics and Mathematics, Rutgers University, Piscataway, New Jersey,

08855-0849

Abstract

We carried out three-dimensional simulations, with about 1.4×10^6 particles, of phase segregation in a low density binary fluid mixture, described mesoscopically by energy and momentum conserving Boltzmann-Vlasov equations. Using a combination of Direct Simulation Monte Carlo(DSMC) for the short range collisions and a version of Particle-In-Cell(PIC) evolution for the smooth long range interaction, we found dynamical scaling after the ratio of the interface thickness(whose shape is described approximately by a hyperbolic tangent profile) to the domain size is less than ~ 0.1 . The scaling length $R(t)$ grows at late times like t^α , with $\alpha = 1$ for critical quenches and $\alpha = \frac{1}{3}$ for off-critical ones. We also measured the variation of temperature, total particle density and hydrodynamic velocity during the segregation process.

PACS numbers: 64.75.+g, 68.10.-m, 47.70.Nd

Typeset using REVTeX

The process of phase segregation through which a system evolves towards equilibrium following a temperature quench from a homogeneous phase into a two phase region of its phase diagram has been of continuing interest during the last decades [1], but many problems still remain to be solved. This is particularly so for fluids, when particle, momentum and energy densities are conserved locally; these are currently the focus of both numerical studies [2-7] and micro-gravity experiments [8,9].

In this paper we present computer simulations of spinodal decomposition in a three-dimensional mixture of two kinds of particles that we label 1 and 2 using a novel microscopic dynamics and computational scheme. The particles interact with each other through short range interactions modeled here by hard spheres having the same mass m and diameter d . Particles of different kinds interact also through a long range repulsive Kac potential, $V(r) = \gamma^3 U(\gamma r)$. The equilibrium properties of such a system are well understood, there is even a rigorous proof of a phase transition at low temperatures to an immiscible state [10], which in the limit $\gamma \rightarrow 0$ [11], is described by mean field theory. When the density n is low enough, $nd^3 \ll 1$, and the potential sufficiently long ranged, $n\gamma^{-3} \gg 1$, the free energy of the system is well approximated by $F = k_B T \int [n_1(\vec{r}) \ln n_1(\vec{r}) + n_2(\vec{r}) \ln n_2(\vec{r})] d\vec{r} + \int V(|\vec{r}_1 - \vec{r}_2|) n_1(\vec{r}_1) n_2(\vec{r}_2) d\vec{r}_1 d\vec{r}_2$ and the $\gamma \rightarrow 0$ critical temperature, which should be an upper bound for T_c^γ at $\gamma > 0$, is given by $k_B T_c^0 = \frac{1}{2} n \int U(r) d\vec{r}$. In this regime the dynamical evolution of the system should be well described by two coupled Boltzmann - Vlasov equations:

$$\frac{\partial f_i}{\partial t} + \vec{v} \cdot \frac{\partial f_i}{\partial \vec{r}} + \frac{\vec{F}_i}{m} \cdot \frac{\partial f_i}{\partial \vec{v}} = J[f_i, f_1 + f_2], \quad i = 1, 2 \quad (1)$$

where $f_i(\vec{r}, \vec{v}, t)$ are the one-particle distribution functions, $\vec{F}_i(\vec{r}, t) = -\nabla \int V(|\vec{r} - \vec{r}'|) n_j(\vec{r}') d\vec{r}'$, $n_j(\vec{r}) = \int f_j(\vec{r}, \vec{v}, t) d\vec{v}$ with $i, j = 1, 2, i \neq j$, and $J[f, g]$ is the Boltzmann collision operator for hard core interactions [14]. Kinetic equations of this type have been proposed in [12], and if the system is quenched inside the coexistence region they will describe gas-gas segregation [13] into two phases, one rich in particles of type 1 and the other rich in particles of type 2. (Examples of gas mixtures that have a miscibility gap are helium-hydrogen, helium-nitrogen, neon-xenon etc. [13].) We believe that the model contains the

essential features of phase separation in general binary fluid mixtures.

To simulate our system we modeled the Boltzmann collisional part using a stochastic algorithm due to Bird [15], known as Direct Simulation Monte Carlo (DSMC), while for the Vlasov part we used the particle-to-grid-weighting method, well known in plasma physics [16]. In the DSMC method the physical space is divided into cells containing typically tens of particles. The main ingredients of this procedure are the alternation of free flow over a time interval Δt and representative collisions among pairs of particles sharing the same cell. In the particle-to-grid-weighting algorithm the particle densities are computed on a spatial grid through some weighting depending on the particle position, then the Vlasov forces are calculated on the same grid. Finally, the forces at the position of each particle are interpolated from the forces on the grid. The coupling of these methods, which have been extensively used individually, made possible our simulations of phase segregation with 1.4×10^6 particles, with only modest computational resources: a typical run took about 32 CPU hours on a 233 MHz Alpha Station. It appears that this method can be extended to the study of the effects of phase segregation on inhomogeneous hydrodynamical flows of practical importance [17].

Since one of our main interests was the late time hydrodynamical regime, a delicate balance had to be struck between the size of the system, the range of the potential, the temperature and the particle density, making sure that each of the methods is used within its range of validity and that their combination remains computer manageable. On the one hand the potential must be reasonably long ranged so that the Vlasov description is physically appropriate and numerically sound, and on the other hand it must have a range much smaller than the size of the system. This restriction made necessary the use of two spatial grids: a somewhat coarse one for the collisions and a finer grid for the long range potential. It also imposed the use of quadratic spline interpolation for the calculation of grid quantities and a ten-point difference scheme for the calculation of the forces [16].

Our results were obtained using a system with 1382400 particles in a cube with periodic boundary conditions. We also studied smaller systems to identify unavoidable finite-size

effects. The interaction potential used was gaussian, $U(x) = \alpha\pi^{-\frac{3}{2}}e^{-x^2}$, $\alpha > 0$, but there is no reason to believe that different repulsive potentials would qualitatively change the results. All quenches were performed at a total particle density $nd^3 \simeq 0.01$ and an initial temperature T_0 , $T_0/T_c^0 = 0.5$. The initial conditions for each run were random positions for all particles and velocities distributed according to a maxwellian of constant temperature. (In the DSMC evolution, as in the Boltzmann-Vlasov equations, the hard cores only enter in determining the collision cross sections.) The total energy of the system was very well conserved by the dynamics. This meant that the kinetic energy and hence the temperature increased as the system segregated, but at late times it changed very slowly on the time scale of our simulations. We indicate the final temperature T in the figures. The effective number of particles in the range of the potential was about 100-500.

In the following we compare results of our simulations with available theoretical and experimental work and check various assumptions made in the former, e.g. the neglect of density and temperature variations. We are also currently investigating both formal and rigorous Chapman-Enskog and Hilbert expansion methods for derivation of macroscopic evolution equations for this model [18]. The units used for lengths and times are the mean-free path, $\lambda = (2^{\frac{1}{2}}\pi nd^2)^{-1}$, and mean-free time, $\tau = \lambda/c$, where $c = (2k_B T_0/m)^{\frac{1}{2}}$ and $T_0 = \frac{1}{2}T_c^0$ is the initial temperature.

We first present results for critical quenches (equal volume fractions of the two species). Three different potential ranges were used, and for each one of them 10-12 quenches were performed. The domain size was probed using the pair correlation function, $C(\vec{r}, t) = \mathcal{V}^{-1} \langle \sum_{\vec{x}} \phi(\vec{x}, t) \phi(\vec{x} + \vec{r}, t) \rangle$, where $\phi = (n_1 - n_2)/(n_1 + n_2)$ is the local order parameter, n_1 and n_2 are the local particle densities, \mathcal{V} is the volume and the average is over the different runs. We determined $C(\vec{r}, t)$ by an inverse Fourier transform of the structure function $S(\vec{k}, t) = |\tilde{\phi}(\vec{k}, t)|^2$; the order parameter $\phi(\vec{r}, t)$ and its Fourier transform $\tilde{\phi}(\vec{k}, t)$ were computed on a $64 \times 64 \times 64$ cubic grid. The first zero of the spherically averaged correlation function, $C(r, t)$, was used as a measure of the typical domain size, $R(t)$. The

data are averages of the independent runs.

Assuming the existence of a single characteristic length scale, the dynamical scaling prediction [1] for the late time spherically averaged correlation function is $C(r, t) \simeq C(r/R(t))$. In Fig. 1 the correlation function for potential range $\gamma^{-1} = 0.4$ is plotted starting at $t = 160$, showing that the system is well within the scaling regime.

Simple dimensional analysis of the hydrodynamical evolution equations in the limit of large domain sizes, appropriate for late times, yields a linear growth law for the domain sizes [19], $R(t) \propto (\sigma/\eta)t$, when R is below $R_h = \eta^2/\rho\sigma$ and a $t^{\frac{2}{3}}$ law, $R(t) \propto (\sigma/\rho)^{\frac{1}{3}}t^{\frac{2}{3}}$, for R above R_h [22,23]; σ is the surface tension coefficient, η is the shear viscosity and ρ is the density. We measured σ directly using Laplace's law and η by studying the decay of a sinusoidal velocity profile. The time evolution of $R(t)$ in our simulations is at late times (see Fig. 2) $R(t) = a + b(\sigma/\eta)t$, with $b \simeq 0.13 \pm 0.2$ ($\sigma = 260$ and $\eta = 3250$ for $\gamma^{-1} = 0.4$, $T/T_c^0 = 0.6$). This numerical factor is similar to the one observed in experiments [8] and recent large scale molecular dynamics simulations [7]. Whether or not a crossover to a $t^{\frac{2}{3}}$ growth occurs at later times/larger domain sizes cannot be decided by our present results. We estimated that we would need a system with at least 4 times as many particles as the present one to be able to observe the growth of domains with sizes bigger than R_h .

The linear regime starts around the time when dynamical scaling begins to hold, i.e. at a domain size of about 12-15 times γ^{-1} , the range of the potential. This is in agreement with Siggia [19] who argued that the linear regime is due to surface tension driven flows, so the interfaces should be well defined, i.e. their width should be small compared to the domain size. This width is usually taken to be of order ξ , the correlation length of order parameter fluctuations in the bulk phases. One expects ξ to be roughly equal to γ^{-1} , far away from the critical temperature, as we are [20].

We also looked directly at the wall profiles separating different phases and found that they are approximately described by solitonic solutions [21]. These are particle densities $n_i(z)$ depending on a single spatial coordinate, such that $f_i(z, \vec{v}) = n_i(z)\exp(-mv^2/2k_B T)$ are stationary solutions of Eq.(1) and $n_1(\pm\infty) = n_2(\mp\infty)$ are the mean-field equilibrium

densities at temperature T . The order parameter profiles which satisfy the equation and the ones observed in the simulations (see Fig. 4) have both approximately the hyperbolic tangent form [20], $\tanh(z/2\xi)$, with z the coordinate perpendicular to the domain wall and ξ a parameter which characterizes the interface thickness. We found that this thickness is about 50 percents bigger than γ^{-1} . The total density is about 20 percents smaller (for $\gamma^{-1} = 0.4$, $T/T_c^0 = 0.6$) at the interface than in the bulk, in very good agreement with the solitonic solution (see Fig. 4). The solitonic profiles were calculated at an effective temperature T_{eff} for which the asymptotic values of the order parameter matched the ones observed in the simulations. These asymptotically matched mean-field profiles are steeper (in units of γ^{-1}) than the ones observed, with better agreement as γ is decreased. We believe that this discrepancy is due to the fact that $T/T_c^\gamma > T_{eff}/T_c^0$, as the equilibrium curve for $\gamma > 0$ is flatter around T_c than the mean-field curve.

The need for a clear separation between boundary width and domain size may explain why in earlier molecular dynamics simulations [2], a smaller exponent is found: in those computations the maximum domain size observed is only 6-8 times the range of the potential, so the true hydrodynamic regime was probably never reached. In simulations using the lattice Boltzmann method the interaction range is of the order of one lattice spacing and the hydrodynamic exponent is observed when the domain size is about 10 lattice units [4], in agreement with our analysis.

At early times the growth is consistent with a $t^{\frac{1}{3}}$ behavior, for all potential ranges [19,24]. This exponent is not associated with a scaling regime and it may not be universal, but it is not inconsistent with the experimental results [8,9]. In fact, we were able to collapse the three curves onto each other through scaling of the lengths and times Fig. 2 [6].

Off-critical quenches were performed for a single range of the potential and three volume fractions. To our knowledge no published results of such simulations exist, although they are mentioned in [7]. Therefore, we compare our results to recent experimental work [9] and analyze them using the known coarsening mechanisms [19,25]. In Fig. 3 we present the domain growth for $\gamma^{-1} = 0.4$ and volume fractions 0.16, 0.22 and 0.28. We plot $R^3(t)$ vs. t ,

and the late times regime is clearly consistent with a $\frac{1}{3}$ exponent. In this regime the system satisfies dynamical scaling very well. The presence of a late times $t^{\frac{1}{3}}$ growth at volume fractions less or equal than about 0.3 was observed recently in micro-gravity experiments [9] and reasonably explained theoretically using a droplet coalescence mechanism [19,25]. This regime was also analyzed by Siggia who predicted a prefactor proportional to $v^{\frac{1}{3}}$ (v being the volume fraction of the minority species). In our simulations the prefactors are in reasonable agreement with the above prediction. Furthermore, we can clearly see the motion and coalescence of the droplets in movies of the dynamics.

In writing down evolution equations for the order parameter and velocity fields in a symmetric binary system with momentum and energy conservation it is generally assumed that the density and temperature variations are small [26]. We were able to check these quantities directly by dividing the system into 'hydrodynamical' cells, each containing about 100 particles, and computing the order parameter, density, temperature ($k_B T \equiv \frac{1}{3} m (\langle \vec{v}^2 \rangle - \langle \vec{v} \rangle^2)$, averages over the cell) and fluid velocity in each cell. While the statistical fluctuations of these quantities are not vanishingly small, as they should be for true hydrodynamic variables, they are small enough for such a description to be at least reasonable. As already mentioned the total density is smaller at the boundary between domains. Away from the domain boundaries the values of the density and order parameter were close to their equilibrium values. The temperature appeared to be uniform, with normal equilibrium fluctuations everywhere in the system. This shows that the time scales over which heat transport takes place are much smaller than the time scales over which there is significant phase separation.

If, as argued, the linear growth regime is due to surface tension driven flows, one would expect bigger hydrodynamic velocities close to the interfaces than in the bulk. We looked therefore at the distribution of hydrodynamic velocities as a function of the order parameter for critical quenches. As the system segregates, bigger hydrodynamic velocities are typically observed close to the domain walls, identified by small values of the order parameter. While this may be due in part to the density being smaller at the boundary between domains, it is also consistent with the idea that at late times the flows are generated mainly by the

curvature of well formed interfaces. We are planning to study this issue more carefully using bigger systems.

A natural refinement of our model would be the use of the Enskog correction for the collisions [14](which would require numerically replacing the DSMC part with its recently proposed extension [27], the Consistent Boltzmann Algorithm(CBA)) and of long range attractive forces between like particles.

We believe that we have introduced a new model which is closer to reality than lattice gases usually simulated, but still tractable numerically by the new techniques that we have introduced. These techniques are of independent interest and have enabled us to compute temperature changes, density variations and profiles not done before. Furthermore, we can compare our results to some exact ones. In fact, we think that this model is a paradigm for the rigorous derivation of hydrodynamic equations.

We would like to thank Frank Alexander for useful discussions. This research was supported in part by AFOSR Grant 0159 and NSF Grant 92-13424.

REFERENCES

- [1] J.D. Gunton, M. San Miguel and P.S. Sahni, in *Phase Transitions and Critical Phenomena*, vol.8, edited by C. Domb and J.L. Lebowitz(Academic, New York, 1983); A.J. Bray, *Adv. Phys.* **43**, 357, (1994).
- [2] Wen-Jong Ma, A. Maritan, J. Banavar and J. Koplik, *Phys. Rev. A*, **45**, R5347, (1992).
- [3] O.T.Valls and J.E.Farrell, *Phys. Rev. E* **47**, R36, (1993); A. Shinozaki and Y.Oono, *Phys. Rev. E.* **48**, 2622, (1993).
- [4] F.J. Alexander, S. Chen and D.W. Grunau, *Phys. Rev. B* **48**, 634, (1993).
- [5] Y. Wu, F.J. Alexander, T. Lookman and S. Chen, *Phys. Rev. Lett.* **74**, 3852, (1995); T. Lookman, Y. Wu, F.J. Alexander and S. Chen, *Phys. Rev. E*, **53**, 5513, (1996).
- [6] S. Bastea and J.L. Lebowitz, *Phys. Rev. E*, **52**, 3821, (1995).
- [7] M. Laradji, S. Toxvaerd and O.G. Mouritsen, *Phys. Rev. Lett.*, **77**, 2253, (1996).
- [8] P. Guenoun, R. Gastaud, F. Perrot and D. Beysans, *Phys. Rev. A*, **36**, 4876, (1987).
- [9] F. Perrot, P. Guenoun, T. Baumberger and D. Beysens, *Phys. Rev. Lett.* **73**, 688, (1994); Y. Garrabos, B. Le Neindre, P. Guenoun, B. Khalil and D. Beysans, *Europhys. Lett.*, **19**, 491, (1992).
- [10] J.L. Lebowitz and E.H. Lieb, *Phys. Lett.* **39A**, 98, (1972).
- [11] J.L. Lebowitz and O. Penrose, *J. Math. Phys.* **7**, 98, (1966).
- [12] Luis De Sobrino, *J. Can. Phys.*, **45**, 363, (1967); M. Grmela, *J. Stat. Phys.*, **3**, 347, (1971).
- [13] J.A. Schouten, *Phys. Rep.* **172**, 33, (1989).
- [14] S. Chapman and T.G. Cowling, *The Mathematical Theory of Non-uniform Gases*, (Cambridge University Press, 1970).

- [15] G.A. Bird, *Molecular Gas Dynamics*, (Clarendon Press, Oxford, 1976).
- [16] C.K. Birdsall and A.B. Langdon, *Plasma Physics Via Computer Simulation*, (McGraw-Hill Book Company, New York, 1985).
- [17] R.E. Goldstein, A.I. Pesci and M.J. Shelley, Phys. Rev. Letters, **70**, 3043, (1993).
- [18] S. Bastea, R. Esposito, J.L. Lebowitz and R. Marra, in preparation.
- [19] E.D. Siggia, Phys. Rev. A **20**, 595, (1979).
- [20] J.S. Rowlinson and B. Widom, *Molecular Theory of Capillarity* , (Clarendon Press, Oxford, 1982).
- [21] G. Giacomin and J.L. Lebowitz, Phys. Rev. Lett., **76**, 1094, (1996).
- [22] H. Furukawa, Physica A, **204**, 237, (1994).
- [23] S. Bastea and J.L. Lebowitz, Phys. Rev. Lett. **75**, 3776, (1995).
- [24] A.Z. Akcasu and R. Klein, Macromolecules **26**, 1429, (1993).
- [25] V.S. Nikolayev, D. Beysens and P. Guenoun, Phys. Rev. Lett., **76**, 3144, (1996).
- [26] P.C.Hohenberg and B.I.Halperin, Rev. Mod. Phys. **49**, 435, (1977).
- [27] F.J. Alexander, A.L. Garcia and B.J. Adler, Phys. Rev. Lett. **74**, 5212, (1996).

FIGURES

FIG. 1. Scaled two-point correlation function for critical quench with $\gamma^{-1} = 0.4$. Final temperature $T = 0.6T_c^0$.

FIG. 2. Scaled domain growth at critical quench; the $\gamma^{-1} = 0.3$ and $\gamma^{-1} = 0.5$ curves have been collapsed onto the $\gamma^{-1} = 0.4$ curve. A straight line fit($\alpha = 1$) is drawn for late times and a $\propto t^{\frac{1}{3}}$ fit($\alpha = \frac{1}{3}$) is drawn for early times.

FIG. 3. Domain growth for off-critical quenches with $\gamma^{-1} = 0.4$; straight line fits are drawn.

FIG. 4. Total density $n(*)$ and order parameter $\phi(+)$ variations at the interface between the two phases; $\gamma^{-1} = 0.4$ and $T/T_c^0 = 0.6$. The full lines are the solitonic solution(see text).

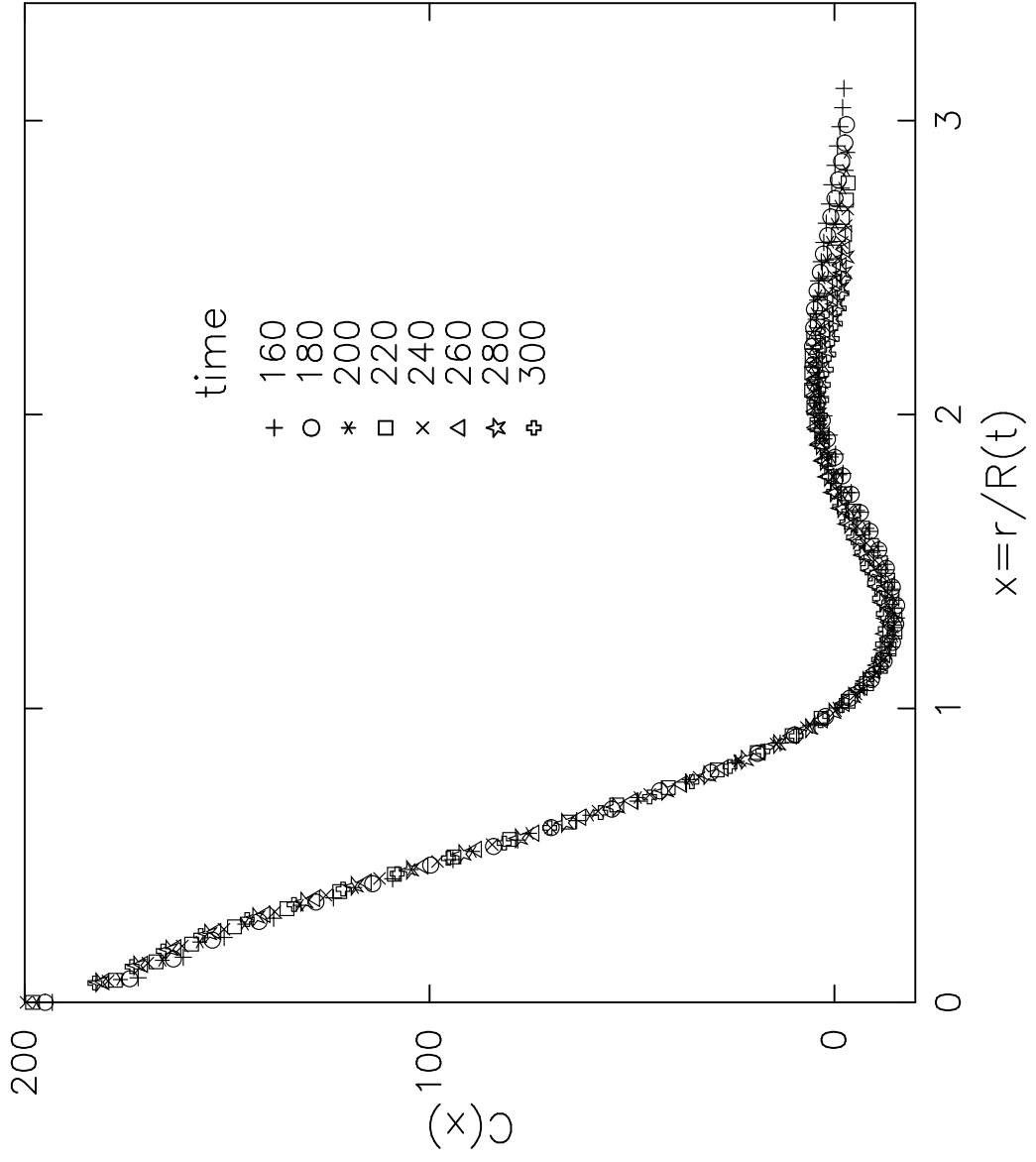


Fig. 1

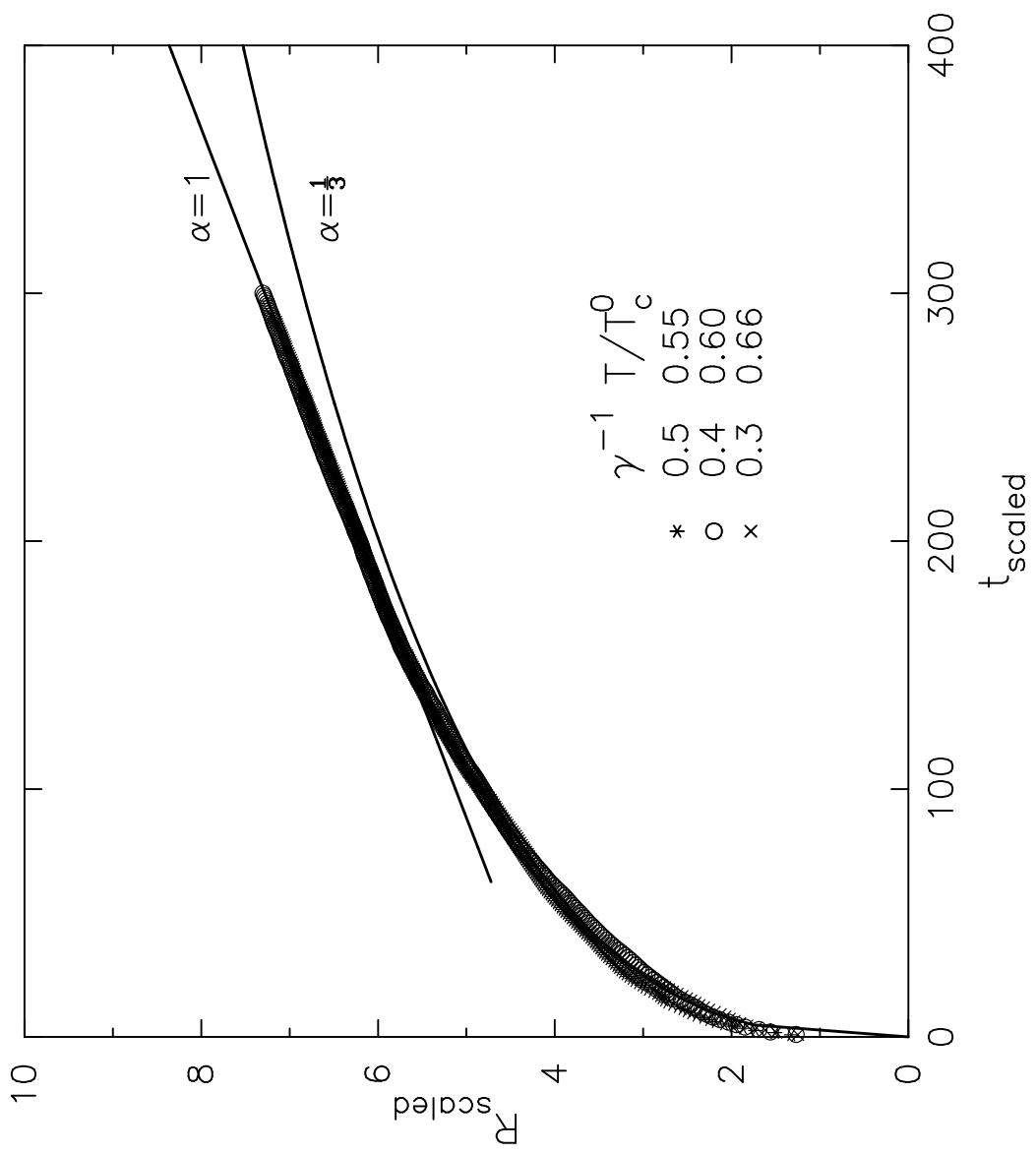


Fig. 2

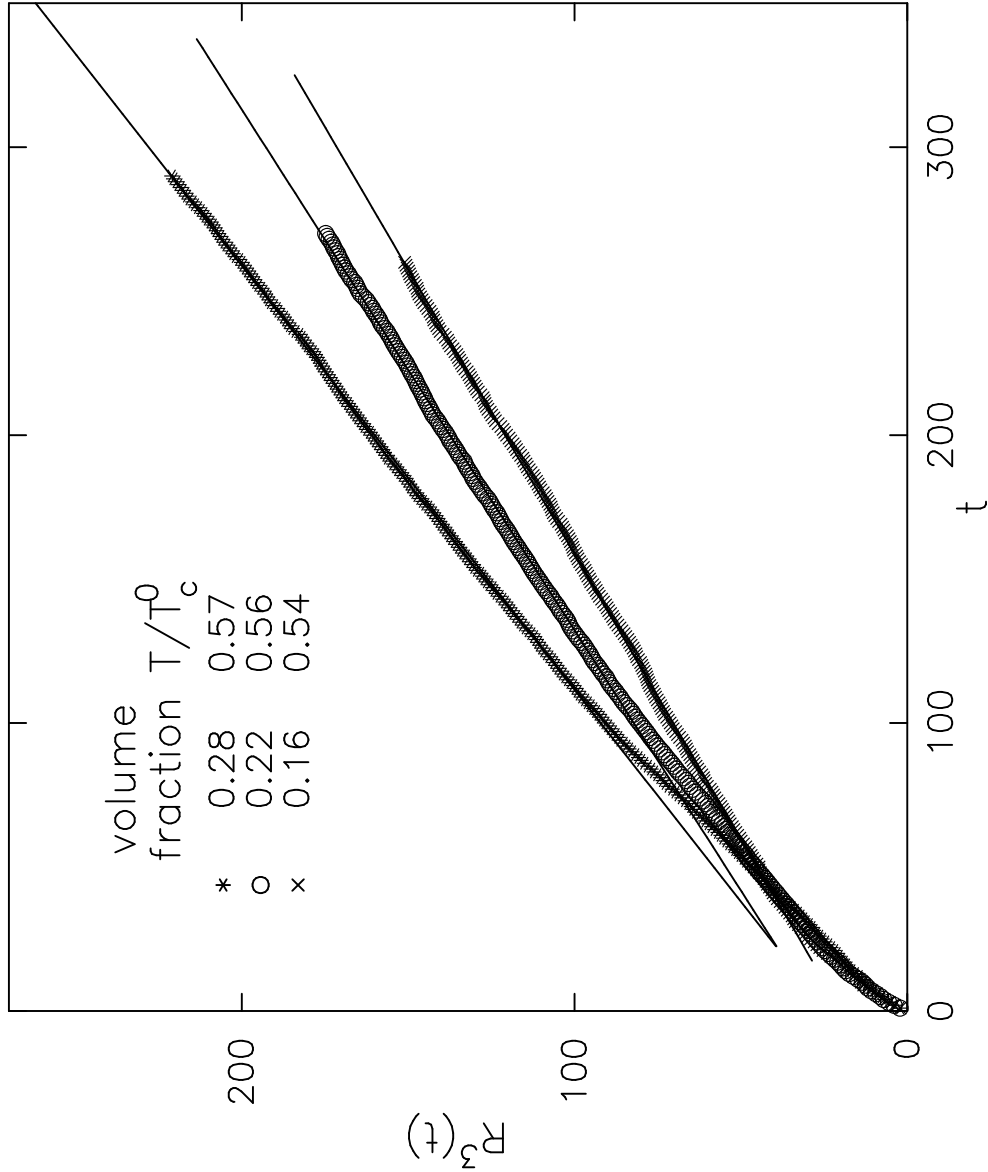


Fig. 3

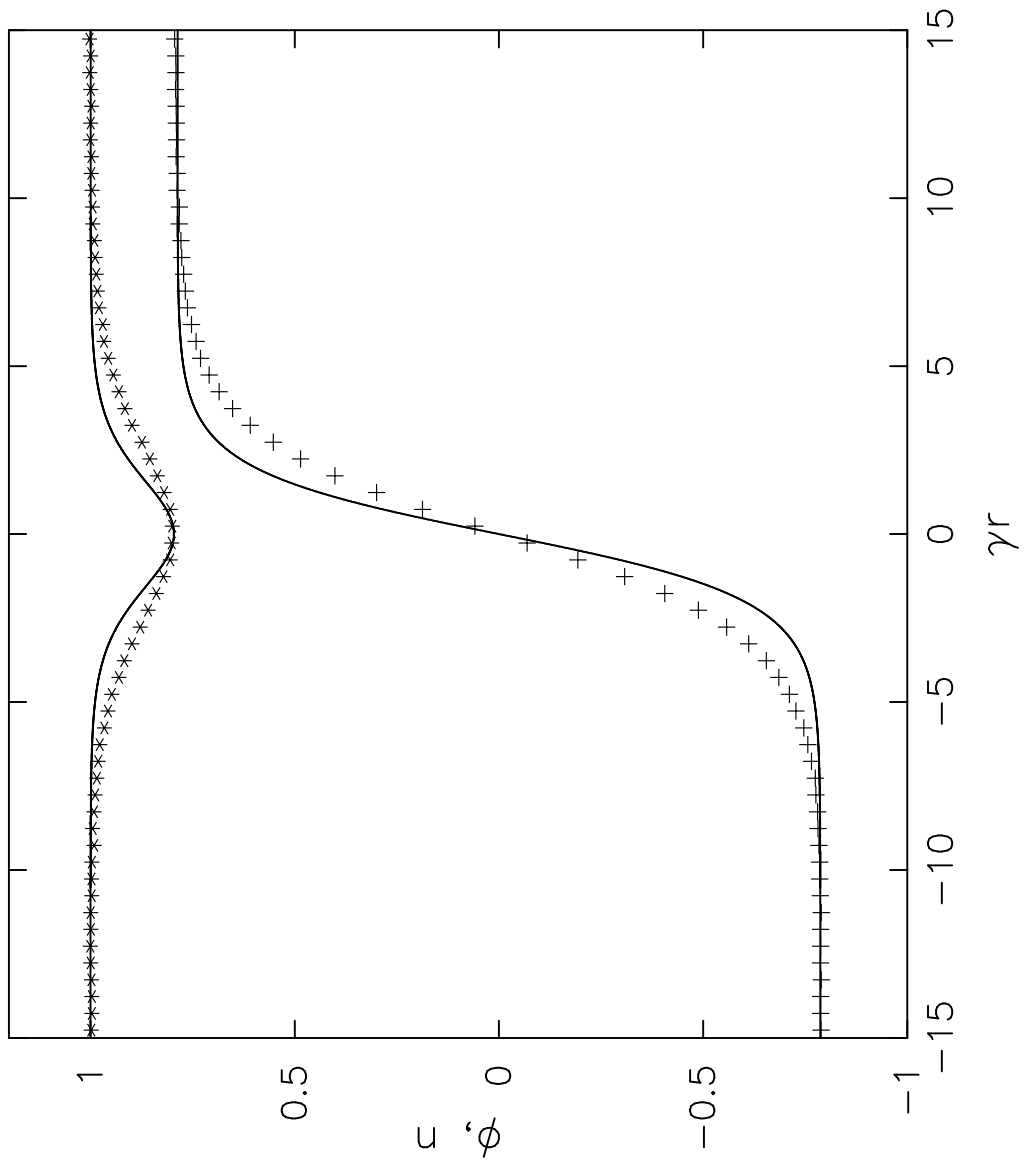


Fig. 4